

Article

Not peer-reviewed version

---

# Identification of TgENT1 as the TgUUT1 Uracil/Uridine Transporter of *Toxoplasma gondii*

---

[Hamza A. A. Elati](#), [Mariana Ferreira Silva](#), [Lilach Sheiner](#)<sup>\*,†</sup>, [Harry P. de Koning](#)<sup>\*,†</sup>

Posted Date: 29 January 2026

doi: 10.20944/preprints202601.2248.v1

Keywords: *Toxoplasma gondii*; nucleoside transporter; uridine transport; 5-fluorouracil; pyrimidine antimetabolite



Preprints.org is a free multidisciplinary platform providing preprint service that is dedicated to making early versions of research outputs permanently available and citable. Preprints posted at Preprints.org appear in Web of Science, Crossref, Google Scholar, Scilit, Europe PMC.

Copyright: This open access article is published under a [Creative Commons CC BY 4.0 license](#), which permit the free download, distribution, and reuse, provided that the author and preprint are cited in any reuse.

Disclaimer/Publisher's Note: The statements, opinions, and data contained in all publications are solely those of the individual author(s) and contributor(s) and not of MDPI and/or the editor(s). MDPI and/or the editor(s) disclaim responsibility for any injury to people or property resulting from any ideas, methods, instructions, or products referred to in the content.

Article

# Identification of TgENT1 as the TgUUT1 Uracil/Uridine Transporter of *Toxoplasma gondii*

Hamza A. A. Elati <sup>1,2,3</sup>, Mariana Ferriera Silva <sup>1,2</sup>, Lilach Sheiner <sup>1,\*,†</sup> and Harry P. de Koning <sup>1,\*,†</sup>

<sup>1</sup> School of Infection and Immunity, College of Medical, Veterinary and Life Sciences, University of Glasgow, Glasgow G12 8TA

<sup>2</sup> Centre for Parasitology, School of Infection & Immunity, Sir Graeme Davies Building, University of Glasgow, Glasgow UK

<sup>3</sup> Department of Pharmacology and Toxicology, Pharmacy College, University of Elmergib, Al Khums, Libya

\* Correspondence: lilach.sheiner@glasgow.ac.uk (L.S.); harry.de-koning@glasgow.ac.uk (H.P.d.K.)

† These authors contributed equally to this work.

## Abstract

The protozoan pathogen *Toxoplasma gondii* is responsible for toxoplasmosis a disease that can be deadly in immunocompromised patients and the developing fetus during pregnancy. Current treatments are widely considered to be suboptimal. We have recently reported that 5-fluoropyrimidines have highly promising anti-toxoplasmosis effects and are taken up by the parasite by a high affinity uracil/uridine transporter, TgUUT1. Here, we attempt to identify the gene encoding this transport protein. The only nucleoside or nucleobase family identified in the *T. gondii* genome was the Equilibrative Nucleoside Transporter (ENT) family, with four members. Of these, TgAT1 is known to be purine-specific, and deletion of the *TgENT2* and *TgENT3* genes, either separately or jointly, did not affect uridine transport or sensitivity to 5-fluoropyrimidines. In contrast, depletion of *TgENT1*, an essential gene, resulted in significant reduction in the uptake of both uracil and uridine but not of the amino acid tryptophan. Moreover, expression of *TgENT1* in a *Leishmania mexicana* cell line with low endogenous uracil uptake rates significantly increased uracil uptake for these cells. We conclude that it is highly probable that *TgENT1* encodes the *T. gondii* uracil/uridine transporter.

**Keywords:** *Toxoplasma gondii*; nucleoside transporter; uridine transport; 5-fluorouracil; pyrimidine antimetabolite

## 1. Introduction

Toxoplasmosis is a common infection of humans and mammals that can be dangerous in its acute form, especially if contracted during pregnancy, as the pathology to the unborn baby can be severe and even fatal [1]. Moreover, chronic infection is thought to persist for life and poses a severe risk to immunocompromised patients [2]. Despite the clinical importance of toxoplasmosis there are still numerous gaps in our knowledge of the biology of its etiological agent, *Toxoplasma gondii*.

*T. gondii* is an apicomplexan parasite and, like other Apicomplexa, including the *Plasmodium* parasites that cause malaria, it is an obligate intracellular parasite [3]. In its tachyzoite form, *T. gondii* is able to invade a broad range of nucleated cell types of almost any warm-blooded animal [4]. Despite its critical dependency on the host for survival our understanding of how the parasite obtains essential nutrients such as nucleotides remains poor.

Like all other parasites, *T. gondii* express highly efficient salvage systems to obtain nutrients from the host environment. This involves the manipulation of nutrient uptake by the host cell [5,6]. Pores in the parasitophorous vacuole membranes allow the diffusion of these nutrients directly to the parasite [7,8], where they are internalized by an array of highly effective nutrient transporters that typically outcompete host transporters in substrate affinity and translocation efficiency.

*Toxoplasma* tachyzoites, like many other parasites, also have high replication rates, requiring large amounts of nucleotides for DNA and RNA synthesis, among other functions. Like all other protozoan parasites where this has been investigated, *Toxoplasma* lack the biosynthesis pathway for purines [9] and thus rely fully on transporters and salvage enzymes for these critical biochemicals. They cannot take up nucleotides like ATP directly from the host cytosol [10] and thus need particularly high affinity transporters to salvage free nucleosides and nucleobases, which are present in low concentrations in the host environment. High affinity transporters for purine nucleosides and oxopurine nucleobases have been described [11].

In contrast, *T. gondii* express the entire pathway for *de novo* pyrimidine synthesis and although this is important for virulence, it is not essential for cellular invasion *in vitro* if the media is supplemented with >20  $\mu$ M uracil [12]. This constitutes functional evidence that *T. gondii* expresses a transporter capable of uracil salvage, and we recently confirmed that uracil and also uridine are indeed readily taken up by *T. gondii* tachyzoites [13], but that its capacity is insufficient to sustain *in vivo* replication.

In recent years, numerous nucleoside and nucleobase transporters of protozoan parasites have been cloned and characterized [14–17] and all were found to be members of the Equilibrative Nucleoside Transporter (ENT) family. Whereas members of the Concentrative Nucleoside Transporter (CNT) family are commonly found in mammalian hosts and many other species [18], none have been found in protozoan genomes. Despite this progress in the characterization of nucleoside and nucleobase transporters, particularly from kinetoplastids and *Plasmodium* species, our understanding of purine and pyrimidine salvage in *Toxoplasma* remains very incomplete.

Apart from their importance in the physiology of protozoan pathogens, transporters have potential as drug targets [19,20]. For *Toxoplasma*, this potential is strongly supported by our recent report showing that the 5-fluoropyrimidines 5-fluorouracil (5-FU), 5-fluorouridine (5F-Urd) and 5-fluoro,2'-deoxyuridine (5F,2'dUrd) are efficiently taken up by *T. gondii* tachyzoites and display 10-fold higher activity against the intracellular parasites than the antifolate sulfadiazine, the 'current gold standard treatment' when combined with pyrimethamine [21]. In a first pilot experiment, 5-FU was at least as effective as sulfadiazine in a mouse model of acute toxoplasmosis [13]. Moreover, the 5-fluoropyrimidines have long been used as anticancer chemotherapy [22] and, according to the one report of their use against acute toxoplasmosis in AIDS patients in combination with the second-line toxoplasmosis drug clindamycin [23], would be safe to use as they are effective at one tenth the dose used against cancer.

Although our previous report identified a new Uracil/Uridine Transporter (TgUUT1), as responsible for uptake of the 5-fluoropyrimidines, the gene encoding this carrier has not yet been identified. Indeed, although the *T. gondii* genome project has long since identified four likely nucleoside or nucleobase transporters of the ENT family (Table 1), only one of the four genes and its product has been characterized: Tg\_244440, which was first identified from a strain made resistant to the adenosine analogue adenine arabinoside (Ara-A), as a low affinity adenosine transporter, and the corresponding protein was therefore named TgAT1 [24]. Recently, we confirmed, by heterologous expression in *Trypanosoma brucei*, that TgAT1 is indeed a low affinity transporter for adenosine but, more surprisingly, it also displayed much higher affinity for the oxopurine nucleobases hypoxanthine and guanine, and their nucleosides inosine and guanosine [25]. Of the three remaining genes encoding putative ENT family members (here collectively called TgENTs), Tg\_288540 is reportedly the only essential gene for *T. gondii* in culture [26] and Tg\_233130 is upregulated in bradyzoites [27].

Here, we start to address the issues raised above, including the role of the TgENTs in pyrimidine uptake, to try to identify the gene encoding TgUUT1, being the carrier for the 5-fluoropyrimidine antimetabolites.

## 2. Materials and Methods

### 2.1. In Vitro Culture of Host Cells and Parasites

#### 3.1.1. *T. gondii* in Human Fibroblasts

The F3 tomato strain (RH  $\Delta$ Ku80 TATi) [13,28], herein referred to as RH, was used as the primary cell line for generation of all the mutant cell lines and also used as control for all the biochemical experiments such as transport assays and drug screening assays, qRT-PCR and plaque assays.

*T. gondii* tachyzoites of the RH and mutant lines were cultured in human foreskin fibroblasts (HFF), sourced from ATCC (SCRC-1041). Parasites were passaged routinely as confluent monolayer of HFF in Dulbecco's Modified Eagle's Medium (DMEM) containing 4.5 gL<sup>-1</sup> glucose, supplemented with 10% (v/v) fetal bovine serum, 4 mM L-glutamine and penicillin/streptomycin antibiotics and grown at 37 °C with 5% CO<sub>2</sub>. Where mentioned anhydrotetracycline (ATc) was added to the medium at a final concentration of 0.5  $\mu$ M.

#### 3.1.2. Leishmania Promastigotes

Three strains of *L. mexicana* promastigote forms were mainly used in this part of the project: **1)** *L. mexicana-Cas9* T7 strain (derived from *L. mexicana* WT promastigotes by expression of the *Streptococcus pyogenes* Cas9 nuclease gene 'Cas9' and maintained on 32  $\mu$ g/mL hygromycin [29], generously donated by Prof. Eva Gluenz (University of Bern, Switzerland). **2)** The *Lmex-NT3-KO* strain ( $\Delta$ NT3) was generated from the *L. mexicana Cas9* strain by CRISPR-mediated deletion of the NT3 transporter gene [30,31]. **3)** The *Lmex-NT3-KO* strain was used as expression system to study TgENT1. All *Leishmania* strains were grown as promastigotes, in standard HOMEM (GIBCO, Life Technologies, Paisley, UK) supplemented with 10% heat-inactivated fetal bovine serum (FBS; PAA Laboratories, Linz, Austria) and 1% of a penicillin–streptomycin solution (Life Technologies) at 25 °C, as described by Al-Salabi, *et al.* [32].

### 3.2. Chemicals and Radiochemicals

Uridine, uracil, thymidine, cytidine, adenosine, Inosine, 5-fluorouracil (5-FU), 5-fluorouridine (5-FUrd), sulfadiazine, resazurin sodium salt and phenylarsine oxide (PAO) were sourced from Sigma-Aldrich (Poole, UK). 5-Fluoro 2'-deoxyuridine (5-F-2'dUrd) was from Avantor (VWR). [2,8-<sup>3</sup>H]-Adenine (40.3 Ci/mmol) was obtained from PerkinElmer (Waltham, MA, USA). [5,6-<sup>3</sup>H]-Uracil (40 Ci/mmol), [5,6-<sup>3</sup>H]-Uridine (60 Ci/mmol), [2,8-<sup>3</sup>H]-Adenosine (40 Ci/mmol) and [<sup>3</sup>H]-Tryptophan (25 Ci/mmol) were sourced from American Radiolabeled Chemicals Incorporated (St Louis, MO, USA).

#### 3.3. Drug Sensitivity Assay for *T. gondii* Tachyzoites

Drug sensitivity assays for *Toxoplasma gondii* tachyzoites were performed as previously described [13]. Briefly, HFF cells were seeded in 96-well black plates and grown to confluence. Test compounds and sulfadiazine (positive control) were prepared in DMEM and serially diluted across the plate, leaving the last column as a drug-free control. Freshly egressed tachyzoites (~1000/well) were added to each well and incubated for 6 days at 37 °C with 5% CO<sub>2</sub>. Fluorescence was measured using a PHERAstar plate reader (excitation: 540 nm; emission: 590 nm). EC<sub>50</sub> values were calculated using GraphPad Prism 10.0 using a 4-parameter sigmoid curve (variable slope). All assays were performed in triplicate and repeated independently 3–5 times.

#### 3.4. Drug Cytotoxicity Assay for HFF Cells Using Alamar Blue Dye

Cytotoxicity was as previously described [13], using PAO as positive control. Plates were incubated for 6 days at 37 °C with 5% CO<sub>2</sub>. On day 6, 10  $\mu$ L resazurin solution (12.5 mg/100 mL ddH<sub>2</sub>O) was added to each well, including media-only wells for background fluorescence. After 3–4 h incubation, fluorescence was measured (excitation: 540 nm; emission: 590 nm) using a PHERAstar

plate reader. Data were analyzed in GraphPad Prism 10.0 using a four-parameter sigmoid curve to calculate EC<sub>50</sub> values. Experiments were performed in triplicate and repeated 3–5 times.

### 3.5. Transport Assays

Transport of radiolabeled uridine, uracil and tryptophan into extracellular *T. gondii* tachyzoites and *L. mexicana* promastigotes was assayed following previously published protocols [11,13,16,31,33]. Briefly, *L. mexicana* promastigotes were grown at 27 °C for 40–48 h to mid-log phase, while *T. gondii* tachyzoites were harvested from confluent HFF cultures maintained at 37 °C and 5% CO<sub>2</sub>. Parasites were washed twice in assay buffer (AB: 33 mM HEPES, 98 mM NaCl, 4.6 mM KCl, 0.5 mM CaCl<sub>2</sub>, 0.07 mM MgSO<sub>4</sub>, 5.8 mM NaH<sub>2</sub>PO<sub>4</sub>, 0.03 mM MgCl<sub>2</sub>, 23 mM NaHCO<sub>3</sub>, 14 mM D-glucose; pH 7.3), counted, and resuspended at 1 × 10<sup>8</sup> cells/mL (*Leishmania*) or 2 × 10<sup>8</sup> cells/mL (*T. gondii*). After 30 min of recovery at room temperature, 100 µL of cell suspension was layered over an oil mixture (1:7 mineral oil:di-*n*-butyl phthalate for *L. mexicana*, 1:5 for *T. gondii*) containing radiolabeled substrate. Incubations were performed for predetermined times and stopped by adding 750 µL of ice-cold stop solution (0.5–2 mM unlabeled substrate). Tubes were centrifuged at 14,800 × *g* for 1 min, flash-frozen, and cell pellets were processed for scintillation counting after SDS lysis. All assays were done in triplicate and repeated in three independent experiments.

### 3.6. Plasmid Construction and Expression of TgENT1 in *L. mexicana* NT3-KO

The *TgENT1* gene was expressed in *L. mexicana* NT3-KO promastigotes (Aldfer et al., 2022b) using the pNUS-HcN plasmid, which carries a neomycin resistance marker (G-418) [34]. The pNUS-HcN vector was digested with *NdeI* and *XhoI* according to the manufacturer's protocol. *TgENT1* was amplified by PCR using Phusion High-Fidelity DNA Polymerase (supplemental Tables S1 and S2). PCR products and digested plasmids were run on 1% agarose gels, visualized under UV light, and purified using the NucleoSpin PCR and Gel Extraction Kit (Macherey-Nagel).

Ligation was performed using the NEBuilder HiFi DNA Assembly Kit (New England Biolabs). The reaction (10 µL total volume) contained 60 ng of digested pNUS-HcN vector and 180 ng of *TgENT1* insert (vector : insert ratio 1:3), combined with 5 µL of NEBuilder HiFi Master Mix and nuclease-free water. The mixture was incubated at 50 °C for 3–4 h. The assembled plasmid was transformed into NEB 5-alpha competent *E. coli* by heat shock. Colonies were selected on LB agar containing 100 µg/mL ampicillin, cultured in LB broth, and plasmid DNA was extracted using the NucleoSpin Plasmid Purification Kit.

Positive clones were screened by Phusion PCR using a *TgENT1*-specific forward primer (HDK-1739) and a pNUS-HcN reverse primer (HDK-340) (listed in Table S3). Confirmation was also achieved by restriction digestion with *NdeI* and *XhoI*, followed by Sanger sequencing (Source Bioscience, Livingston, UK) using (M13F) and gene-specific reverse primers (HDK-1740) (listed in Table S3). Sequence data were analyzed using CLC Genomics Workbench v7.0 (Qiagen). Verified plasmids (pHDK295 'TgENT1') were ethanol-precipitated, and 25 µg of DNA was resuspended in 15 µL sterile water.

Transfection was performed as described [31]. Briefly, 5 × 10<sup>7</sup> *L. mexicana* NT3-KO promastigotes were harvested, washed twice in PBS, and resuspended in 100 µL transfection buffer. Cells were mixed with 10 µg of circular pHDK295 plasmid DNA (episomal expression) or RNase-free water (negative control), transferred to a 0.2 cm cuvette, and electroporated using the Amaxa Nucleofector (Program U-033). Cells were recovered overnight in HOMEM medium supplemented with 10% FBS at 25 °C, followed by selection with 50 µg/mL G-418. Cultures were plated by limiting dilution (1:10, 1:25, 1:100) in 96-well plates and incubated at 25 °C for 10–14 days to obtain individual clones. Positive clones were expanded in HOMEM medium containing G-418. Genomic DNA was extracted using the NucleoSpin Tissue Kit (Macherey-Nagel), and integration was confirmed by PCR using *TgENT1*-specific forward (HDK-1739) and pNUS-HcN reverse primers (HDK-340).

### 3.7. CRISPR-Mediated Gene Disruption in *T. gondii* Tachyzoites

#### 3.7.1. Direct Gene Knockout

Plasmids for gene knockout and knockdown were constructed using CRISPR-guided promoter replacement in *T. gondii* RH tomato  $\Delta$ Ku80 TATi cells (herein called RH cell line) as described previously [28,35]. Three plasmids were used for these strategies: (i) pDTS4-DHFR for non-essential gene replacement or promoter replacement for essential genes [28]; (ii) an mNeonGreen cassette plasmid for homologous recombination knockout [36]; and (iii) pg474 (Tub-Cas9-YFP-pU6-ccdB-tracrRNA) for delivery of sgRNA/Cas9 [35]. The pDTS4-DHFR plasmid was used to generate two single knockout strains, of *TgENT2* and *TgENT3*, and knockdown of *TgENT1*, while the mNeonGreen cassette was used to generate a double knockout (targeting *TgENT2* in a  $\Delta$ *TgENT3* background) and  $\Delta$ *TgAT1* in the RH strain.

Single guide RNAs targeting the start codon region of *TgAT1*, *TgENT1*, *TgENT2*, and *TgENT3* were designed using the ChopChop online website tool (<https://chopchop.cbu.uib.no/>) and are listed in (Supplemental Table S4). Each sgRNA was cloned into pg474 via *BsaI* restriction sites. Plasmids were purified using Qiagen Miniprep and Midiprep kits according to the manufacturer's instructions. The DHFR cassette allowed selection for pyrimethamine resistance [28], while mNeonGreen-positive parasites were selected by fluorescence-activated cell sorting (FACS). PCR primers for cassette amplification and diagnostic PCR are listed in (Supplemental Table S5). Homology regions for DHFR cassettes were 50 bp at the 5' and 3' UTRs of the target gene, while mNeonGreen cassettes used 40 bp homology regions. PCR products were confirmed by agarose gel electrophoresis and purified using QIAquick PCR Purification kit (Qiagen) prior to transfection.

#### 3.7.2. Gene Knockdown (Tetracycline-Inducible Transactivator System)

Gene knockdown constructs were generated using the same CRISPR/Cas9 workflow described above for Direct Gene Knockout, with modifications to incorporate the ATc-repressible T7S4 promoter. Single guide RNAs targeting the start codon region of *TgENT1* were designed using ChopChop online website tool and are listed in (Supplemental Table S1). Each sgRNA was cloned into pg474 via *BsaI* restriction sites as described for knockout. The DHFR/T7S4 cassette was amplified from pDTS4-DHFR using primers bearing 50 bp homology to the *TgENT1* locus (Supplemental Table S5). PCR reactions were performed with Platinum SuperFi II DNA Polymerase (Supplemental Tables S6&S7), products were verified by agarose gel electrophoresis and purified using the QIAquick PCR Purification kit (Qiagen). Plasmids were prepared using Qiagen miniprep/midiprep kits according to the manufacturer's instructions.

#### 3.7.3. Transfection and Selection

Transfections were carried out using freshly egressed tachyzoites. Briefly,  $1-5 \times 10^6$  parasites were resuspended in Cytomix (120 mM KCl, 0.15 mM CaCl<sub>2</sub>, 25 mM HEPES, 5 mM MgCl<sub>2</sub>, 10 mM K<sub>2</sub>HPO<sub>4</sub>/KH<sub>2</sub>PO<sub>4</sub>, pH 7.6) supplemented immediately before use with 65  $\mu$ l of 3 mM ATP and 65  $\mu$ l of 3 mM glutathione. Approximately  $\sim$ 50  $\mu$ l of purified PCR cassette and 50–70  $\mu$ g of sgRNA/Cas9 plasmid were added (total electroporation volume  $\sim$ 0.8 mL in a 4 mm cuvette). Electroporation was performed using a square-wave protocol (1700 V, 0.2 ms pulse length, two pulses separated by 5 s). Parasites were transferred to confluent HFF monolayers and incubated at 37 °C with 5% CO<sub>2</sub>. Integration events using DHFR were selected with pyrimethamine (1  $\mu$ M) within 24 h for 5–8 days. Once the drug-selected parasites grow out (5–7 days), a 96-well plate of HFF cells was used for cloning the pool by serial dilution. Correct integration and promoter replacement were verified by diagnostic PCR (Supplemental S8 and S9) using primers listed in Table S5; knockdown efficiency was assessed by qRT-PCR where indicated using primers listed in Table S10.

### 3.7.4. Fluorescence-Activated Cell Sorting

For constructs incorporating mNeonGreen (e.g., enrichment of double knockout pools and  $\Delta$ TgAT1 pool), transfected parasites were allowed to recover for ~48 h, then released, passed through a 26 G needle, and a 3  $\mu$ m filter. The parasites were collected and centrifuged for 10 min at RT. The supernatant was discarded and resuspended in FACS buffer (1% Fetal calf serum, 1 mM EDTA in PBS) at roughly  $10^7$ /mL and 1–2 mL transferred to FACS tubes. The transfected samples, including positive control (green), negative control sample (red tomato), sorted on a high-speed cell sorter (BD FACSAria IIu or BD FACSAria III high-speed cell sorter). Gating was established using non-transfected (RH) and mNeonGreen-positive controls. Single fluorescent parasites were sorted directly into 96-well plates pre-seeded with HFFs and cultured at 37 °C/5% CO<sub>2</sub> for 5–7 days to obtain single clonal plaques. Single clones were confirmed by PCR and qRT-PCR using primers listed in Tables S5 and S10.

### 3.8. Plaque Assay

Plaque assays were performed to assess parasite growth as described previously [37]. Confluent HFF monolayers in 6-well plates were infected with freshly egressed tachyzoites (100 parasites per well). Parasites were grown in the presence or absence of anhydrotetracycline (ATc, 0.5  $\mu$ M) and incubated at 37 °C with 5% CO<sub>2</sub> for 7 days without agitation. After incubation, wells were examined by light microscopy to confirm plaque formation. Cells were fixed by adding 300  $\mu$ L of ice-cold 100% methanol per well and incubating for 20 min at room temperature. Fixed monolayers were washed three times with PBS and stained with 2 mL of 0.4% crystal violet solution for ~2 h at room temperature. Wells were washed three times with PBS, air-dried, and plaques were imaged.

### 3.9. Quantitative Real Time PCR (qRT-PCR) in *T. gondii* Tachyzoites

qRT-PCR was carried out as previously described [38,39], to assess gene expression changes. Specifically, qRT-PCR was used to measure the expression level of mRNA for TgENT1 downregulation upon ATc treatment, to confirm the deletion of *TgAT1*, *TgENT2*, *TgENT3*, and the double knockout (DK) lines, and to evaluate potential upregulation or downregulation of TgENT genes in each knockout line. qRT-PCR primers were designed using NCBI Primer-BLAST website [Primer designing tool](#) (Supplemental Table S10). For knockdown experiments, parasites were grown in the presence or absence of ATc for 24, 48, or 72 h; for knockout lines, parasites were grown without ATc. Parasites were collected, passed through a 3  $\mu$ m polycarbonate filter, and pelleted by centrifugation at 1500  $\times$  g for 10 min at RT. Total RNA was extracted using the RNeasy Mini Kit (Qiagen) with on-column DNase I treatment (Thermo Fisher) according to the manufacturer's instructions. cDNA was synthesized using the High-Capacity RNA-to-cDNA Kit (Applied Biosystems). qRT-PCR reactions were set up with Power SYBR Green PCR Master Mix (Applied Biosystems) using 10 ng of cDNA as template and gene-specific primers (listed in Table S10). Reactions were run on a 7500 Real-Time PCR System (Applied Biosystems) under standard cycling conditions. Relative expression was calculated using the  $2^{-\Delta\Delta C_t}$  method [40], using catalase mRNA as the internal control. Three independent biological replicates were performed for each condition, and data were analyzed and plotted using GraphPad Prism 10.0.

### 3.10. qRT-PCR for *L. mexicana* Promastigotes

qRT-PCR was performed as previously described [31,41] to determine the expression levels of TgENT1 in Lmex-NT3-KO compared to the control line and to select the optimal clone. RNA was extracted from *L. mexicana* promastigotes ( $2 \times 10^6$  cells/mL) using the NucleoSpin RNA kit (Macherey-Nagel, Düren, Germany) according to the manufacturer's instructions and quantified using a NanoDrop ND-1000 spectrophotometer. Samples were stored at -80 °C until further use. qRT-PCR primers were designed using NCBI Primer-BLAST website [Primer designing tool](#) (Supplemental Table S10). cDNA was synthesized from 2  $\mu$ g of RNA using the Precision nanoScript II Reverse

Transcription kit (PrimerDesign Ltd., Eastleigh, UK) following the manufacturer's protocol and stored at  $-20^{\circ}\text{C}$ . Primer efficiency was determined using the Pfaffl method [42]. Amplification was performed using the PrecisionPLUS OneStep RT-qPCR Master Mix kit (PrimerDesign Ltd., Eastleigh, UK) with SYBR Green on a 7500 Real-Time PCR System (Applied Biosystems, Thermo Fisher Scientific, Oxford, UK). Cycling conditions were:  $50^{\circ}\text{C}$  for 2 min,  $95^{\circ}\text{C}$  for 10 min, followed by 45 cycles of  $95^{\circ}\text{C}$  for 15 s and  $60^{\circ}\text{C}$  for 1 min. A dissociation curve was included to confirm single-product amplification. Negative controls included samples without reverse transcriptase or cDNA. Gene expression was normalized to GPI8, a constitutively expressed housekeeping gene in *L. mexicana* [43]. Relative quantification was calculated using the  $2^{-\Delta\Delta\text{Ct}}$  method, and data analysis was performed using Applied Biosystems 7500 Fast Real-Time PCR System Software. Each experiment was carried out in triplicate with three independent biological replicates, and data were analyzed and plotted using GraphPad Prism 10.0.

### 3. Results

#### 3.1. Creation of TgENT Knockout (KO) and Knockdown (KD) Strains

##### 3.1.1. Identification of Toxoplasma ENTs

We performed protein-protein BLAST or position-specific iterated BLAST on ToxoDB (<https://toxodb.org/toxo/app>) using human (ENT1-4, CNT1-3) or *Plasmodium falciparum* (ENT1-4) nucleoside transporter genes as query sequences to search for *Toxoplasma* homologs. Consistent with similar queries of other protozoan genomes [14,44], no homologs of human CNTs were identified in any of the genomes accessible through ToxoDB (<https://toxodb.org/toxo/app>). However, the searches identified four genes in the *Toxoplasma* genome with ENT homology, that are numbered as follows in the ME49 genome: TGME49\_233130, TGME49\_244440, TGME49\_288540, and TGME49\_500147. Of these, gene TGME49\_244440 was previously proposed to be an Adenosine Transporter (TgAT1) [24] and we propose to keep that name so as not to confuse the literature although we have shown that this gene encodes a transporter with much higher affinity for oxopurines than for adenosine [25]. The other genes were given an NT1 – NT3 numbering in the PhD thesis by Kshitiz Chaudhary of the research group of David Roos [45] and we propose, again, to keep the same numbering, but naming the genes TgENT1 – 3 (Table 1), as the function of these genes has not been established yet. While they are likely members of the ENT gene family, nucleoside transporter activity was not demonstrated at this point. This naming is also consistent with a recent paper by Messina, Goerner, Bennett, Brennan, Carruthers and Martorelli Di Genova [26] and while a paper describing the cellular localization of some of the *T. gondii* nucleoside transporters [46] provided slightly different names, we propose to consolidate according to the current majority here (Table 1).

Table 1. ENT genes.

<i>T. gondii</i> Gene ID		Name	bp (no introns)	a.a.	TMD*	Qian et al
TGME49	TGGT1					
244440	244440	TgAT1	1389	462	10	TgAT1
288540	288540	TgENT1	2091	696	10	TgNT1
500147	359630	TgENT2	2007	668	10	TgNT3
233130	233130	TgENT3	1596	531	10	TgNT2

Data according to ToxoDB release 68, accessed 10 December 2025. \*, <https://services.healthtech.dtu.dk/services/TMHMM-2.0/>.

##### 3.1.2. Construction of TgENT2 and TgENT3 Knockouts in *T. gondii* RH Cell Line

In order to generate the tools to identify which one of the TgENT genes may encode the previously described Uracil/Uridine Transporter TgUUT [13], we opted to use genetic deletion of TgENT2 and TgENT3 in the *T. gondii* RH background. Likewise, we targeted TgENT1 where all attempt at creating a direct knockout were futile, as predicted in the CRISPR/Cas9 screen [47]

indicating that *TgENT1* is essential for growth in culture, and a conditional knockdown was thus attempted instead; the other three *TgENTs* were found to be non-essential in the same screen and thus direct knock-out (KO) was attempted. Finally, although we have previously characterized *TgAT1* in detail and showed that it is not fully inhibited by even 1 mM uracil or uridine [25], the gene encoding this transporter was also targeted for deletion: (1) in order to confirm the previous observations regarding uracil and uridine, (2) the transporter displayed higher affinity for thymidine than for uracil and 5F-uracil is really a thymine analogue, i.e. it is just possibly that *TgAT1* could take up 5-fluorinated uracil and uridine even though it does not recognize uracil and uridine itself, and (3) to examine the possibility that even if *TgAT1* only displays low affinity and a slow translocation rate for 5-fluoropurimidines, this still could be sufficient for a parasitocidal effect if the parasite is exposed to a drug for a prolonged period [6].

*TgENT2*-KO and *TgENT3*-KO were generated using CRISPR/Cas9 by transfecting RH parasites with the cassette amplified from pDT7S4 template [28] and with Tub-Cas9-YFP-pU6-ccdB-tracrRNA plasmid [35] containing the specific sgRNAs to cut the gene near the start or stop codon, respectively, together facilitating the replacement of the gene of interest (GoI) with the DHFR gene that confers pyrimethamine resistance for selection (Figure 1A,C). Correct integration was confirmed by PCR showing the presence of the ~3.8 kb DHFR amplicon and the absence of the targeted GoI in the transfectants (Figure 1B,D).

The absence of each targeted GoI was further confirmed at the mRNA level using qRT-PCR; gene expression was normalized to the catalase gene expression (Figure 1E,F). In both knockout strains, mRNA of the targeted gene could not be detected but the mRNA level of the other three *TgENTs* was unchanged relative to the parental RH cells (except a minor, just-significant ( $P < 0.05$ , t-test) reduction in *TgENT1* mRNA in the *TgENT2*-KO), suggesting that there was no compensatory upregulation of other transporters after the deletion of either *TgENT2* or *TgENT3*, at least in culture and at the mRNA level.

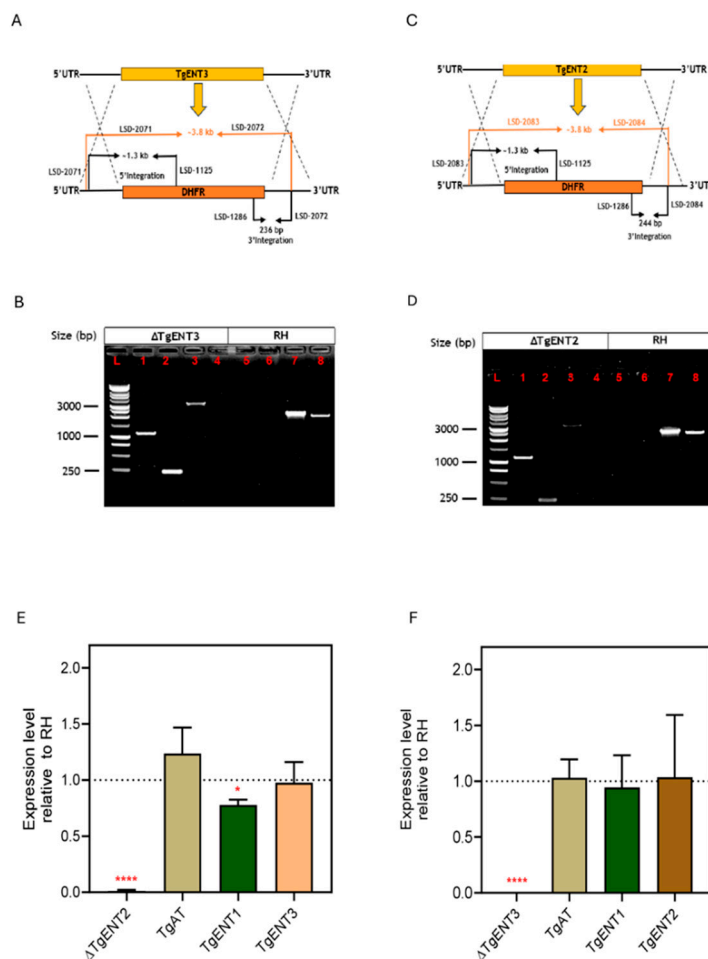


**Figure 1.** Verification of *TgENT3* and *TgENT2* knockout in RH cells. **A.** Schematic depicting the genetic manipulation used to replace *TgENT3* with the DHFR cassette. Primers used in (B) are shown. **B.** PCR confirmation of *TgENT3*-KO of DHFR integration after transfection of the RH cells. (L) 1 kb DNA Ladder; Using the *TgENT3*-KO: (1) LSD-2071-(UTR-F of *TgENT3*) and LSD-1125-DHFR-R; ~1.3 kb; (2) LSD-1286 (DHFR-F) and LSD-2072 (UTR-R of *TgENT3*), 236 bp; (3) LSD-2071-(UTR-F of *TgENT3*) and LSD-2072-(UTR-R of *TgENT3*); ~3.8 kb; (4) LSD-2935 and LSD2936 (open reading frame primers of *TgENT3*); no band. Negative control, RH line: (5) LSD-2071-(UTR-F of *TgENT3*) and LSD-1125-DHFR-R; no band; (6) LSD-2072-(UTR-R of *TgENT3* and LSD-1286-DHFR-F; no band (7) LSD-2071 (UTR-F of *TgENT3*) and LSD-2072 (UTR-R of *TgENT3*); 2.2 kb); (8) LSD-2935 and LSD-2936 ~2 kb. **C.** Schematic depicting the genetic manipulation used to replace *TgENT2* with the DHFR cassette. **D.** PCR Confirmation of *TgENT2*-KO in RH cell line after transfection of the RH cells. (L) 1kb DNA Ladder (Promega); (1) LSD-2083 (UTR-F of *TgENT2*) and LSD-1125 (DHFR-R), ~1.3 kb; (2) LSD-2084 (UTR-R of *TgENT2*) and LSD-1286 (DHFR-F), 244 bp; (3) LSD-2083 (UTR-F of *TgENT2* and LSD-2084 (UTR-R- of *TgENT2*), ~3.8 kb; (4) LSD-2939 and LSD-2940 (ORF primers of *TgENT2*), no band. RH cell line as negative control: (5) LSD-2083 (UTR-F of *TgENT2*) and LSD-1125 (DHFR-R); (6) LSD-2084 (UTR-R of *TgENT2*) and LSD-1286 (DHFR-F); no band (7) LSD-2083 (UTR-F of *TgENT2*) and LSD-2084 (UTR-R of *TgENT2*), ~2.7 kb; (8) LSD-2939-F and LSD-2940-R, ~2.5 kb. **E.** qRT-PCR analysis of *TgENTs* gene expression in the *TgENT2*-KO cell line. **F.** qRT-PCR analysis of *TgENTs* gene expression in the *TgENT3*-KO cell line.

### 3.1.3. Creation of a *TgENT2/3* Double Knockout Cell Line (*ENT2/3dKO*)

An *TgENT2/3dKO* strain was generated using *TgENT3*-KO as the parental line; the mNeonGreen (mNG) cassette [36] was used as a selectable marker for this construct (Figure 2A). A cassette whereby mNG is flanked by the 5'- and 3'-UTRs of *TgENT2* was amplified and transfected into *TgENT3*-KO cells. Transfectants expressing mNG were isolated using flow cytometry. Successful integration in the *TgENT2* locus, was confirmed by PCR reactions (Figure 2B) and the absence of the *TgENT2* and *TgENT3* corresponding mRNAs was confirmed by qRT-PCR (Figure 2C). As in the single gene deletions, there was no significant upregulation of the two remaining *TgENTs* relative to their expression level in RH control cells.

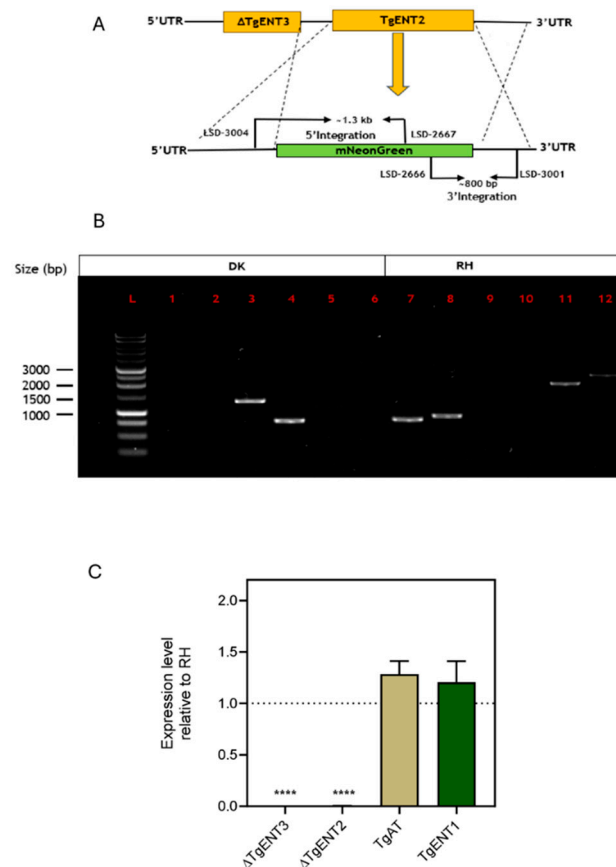


**Figure 2.** Construction and verification of *TgENT2/3dKO* in RH cells. **A.** Schematic for the strategy of making a double knockout of *TgENT2* and *TgENT3*, indicating primer positions. **B.** PCR confirmation of the *TgENT2/3dKO* in RH tachyzoites. L) 1kb DNA Ladder (Promega); (1) LSD-3004-F (5' UTR of *TgENT2*) and LSD-3003-R (downstream start of *TgENT2*), no band; (2) LSD-3002-F (ORF of *TgENT2*) and LSD-3001-R (3' UTR-R of *TgENT2*), no band; (3) LSD-3004 (5' UTR of *TgENT2*) and LSD-2667 (mNG reverse), ~1.3 kb; (4) LSD-2666-F (mNG forward) and LSD-3001-R (3' UTR-R of *TgENT2*), ~800 bp; (5) LSD-2935-F and LSD-2936-R (ORF of *TgENT2*), no band; (6) LSD-2939-F and LSD-2940-R (ORF of *TgENT3*), no band. RH cell line as a negative control: (7) LSD-3004 (5' UTR of *TgENT2*) and LSD-3003-R (downstream start of *TgENT2*), ~750 bp. (8) LSD-3002-F (ORF of *TgENT2*) and LSD-3001-R (3' UTR-R of *TgENT2*), 900 bp. (9) LSD-3004-F (5' UTR of *TgENT2*) and LSD-2667-R (mNG ORF reverse); (10) LSD-2666-F (mNG ORF forward) and LSD-3001 (3' UTR-R of *TgENT2*), ~800 bp; (11) LSD-2935-F and LSD-2936-R (ORF of *TgENT2*), ~2 kb; (12) LSD-2939-F and LSD-2940-R (ORF of *TgENT3*), ~2.5 kb. **C.** qRT-PCR assessment of mRNA levels in *TgENT2/3dKO*.

### 3.1.4. Deletion of *TgAT1* in the RH Cell Line

The knockout of *TgAT1* by CRISPR-assisted homologous recombination and replacement with a DHFR cassette, as for *TgENT2* and *TgENT3* was attempted multiple times but did not yield viable cells upon selection pressure with pyrimethamine, indicating that, at least in our RH strain and under the *in vitro* conditions used, *TgAT1* may essential unlike the other two *TgENTs*. We therefore created a new construct for replacement with mNG, flanked by the *TgAT1* UTRs (Figure 3A). Replacement with this cassette was followed by flow cytometry to isolate positive green fluorescent clones. Correct integration and *TgAT1*-KO were confirmed by PCR reactions (Figure 3B) and mRNA depletion was confirmed by qRT-PCR. Once again, the depletion of *TgAT1* had no significant effect on the mRNA levels of the other *TgENT* genes in support for an absence of compensatory mechanism between those genes in *T. gondii* (Figure 3C).

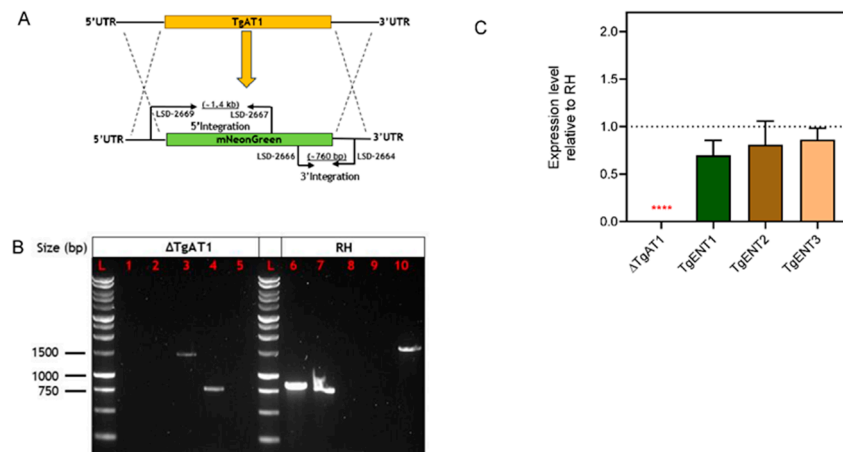


**Figure 3.** Construction and verification of *TgAT1*-KO in RH cells. **A.** Schematic representing the genetic manipulation used to replace *TgAT1* with the mNeonGreen cassette. Primers used in (B) are shown. **B.** PCR confirmation of *TgAT1*-KO using primers of *TgAT1* and mNeonGreen cassette; (L) 1 kb DNA Ladder (Promega); (1) LSD-2669-F (upstream of the start codon of UTR of *TgAT1*) and LSD-2668-R (downstream start codon of *TgAT1*), no band; (2) LSD-2665-F (Upstream of the stop codon of *TgAT1*) and LSD-2664-R (downstream of stop UTR-R of *TgAT1*), no band; (3) LSD-2669-F (upstream of the start codon of UTR of *TgAT1*) and LSD-2667-R (mNeonGreen upstream reverse); band size (~1.4 kb); (4) LSD-2666-F (mNeonGreen downstream forward) and LSD-2664 (downstream of stop codon UTR-R of *TgAT1*); (~760 bp); (5) LSD-2937 and LSD-2938 (ORF of *TgAT1*), no band. RH cell line as a negative control: (6) LSD-2669-F (upstream of the start codon of UTR of *TgAT1*) and LSD-2668-R (downstream start codon of *TgAT1*); Expected band (~860 bp); (7) LSD-2665-F (Upstream of the stop codon of *TgAT1*) and LSD-2664-R (downstream of stop UTR-R of *TgAT1*); Expected band (~796 bp); (8) LSD-2669-F (upstream of the start codon of UTR of *TgAT1*) and LSD-2667-R (mNeonGreen upstream reverse); No band expected in RH control; (9) LSD-2666-F (mNeonGreen downstream forward and LSD-2664 (downstream

of stop codon UTR-R of *TgAT1*); No band expected in RH control; (10) LSD-2937+LSD-2938 (open reading frame of *TgAT1*); Expected band (~ 1.5 kb). C. qRT-PCR analysis of *TgENTs* gene expression in TgAT1-KO cells.

### 3.1.5. Creation of a Conditional Knockout of TgENT1

As mentioned, *TgENT1* is predicted to be essential to tachyzoites *in vitro* [47]. We therefore used promoter replacement (PR) to engineer a conditional depletion line for this gene under control of a tetracycline-inducible transactivator system, illustrated in Figure 4A. This technique relies on replacing the endogenous promoter with the tetracycline responsive promoter T7S4 [28,48]. Primers containing homology to 50 bp stretches of the 5' UTR and the first exon promoted the insertion of the pyrimethamine-resistance (DHFR) cassette for selection followed by the T7S4 promoter that then controls transcription of the native copy of *TgENT1* (Figure 4A) (as described in Lacombe, *et al.* [49]). In this system the addition of anhydrous tetracycline (ATc) binds to the transactivator and prevents transcription, resulting in gene depletion. The resulting manipulation was verified by PCR and after transfection clones with the correct integration of the construct were selected on pyrimethamine and verified by PCR (Figure 4B); the new cell line was named *TgENT1*-KD. Depletion of the corresponding mRNA was tested by qRT-PCR which showed a strong and stable knockdown of mRNA levels as early as 24 h (Figure 4C). Using a plaque assay, we showed that the *TgENT1*-KD cells did not replicate in the presence of ATc, whereas the parental RH cells did (Figure 4D), confirming that *TgENT1* is essential for growth in culture.

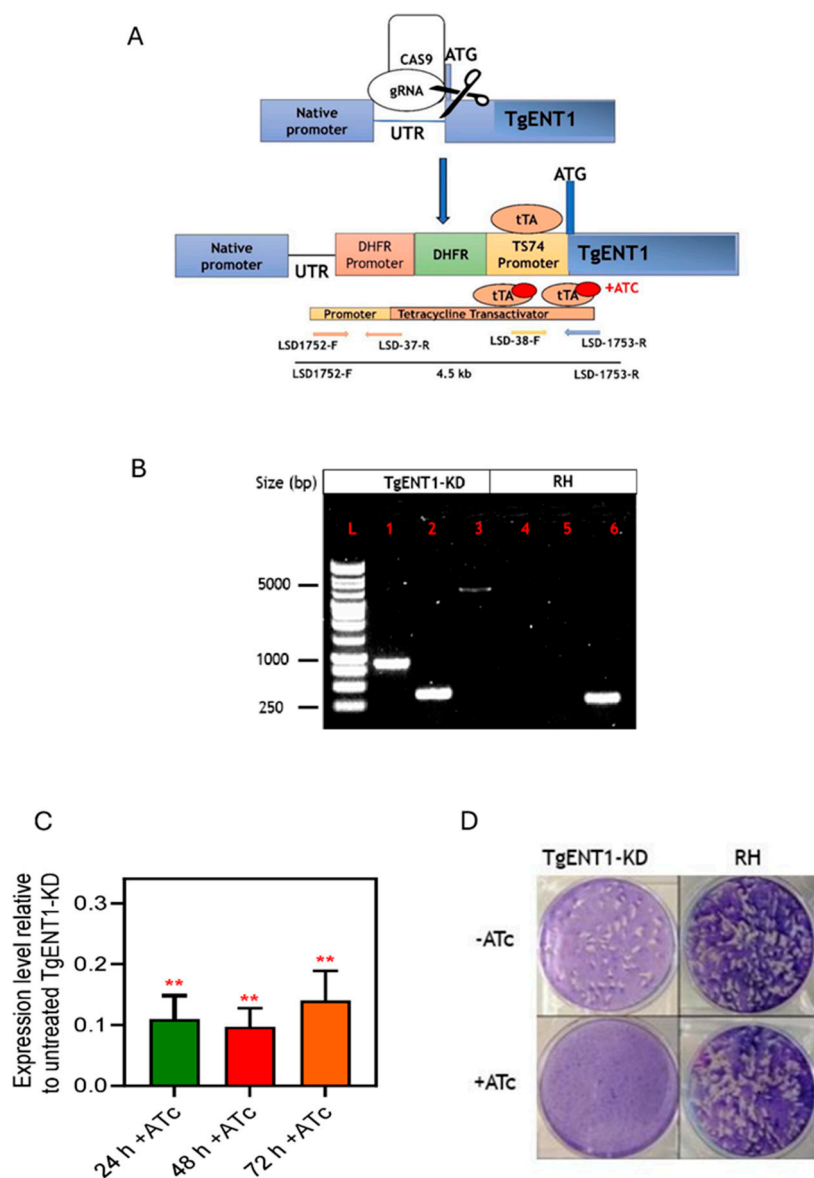


**Figure 4.** Construction and verification of the promoter replacement for *TgENT1*. **A.** Schematic of the CRISPR/cas9-aided strategy for the introduction of the DHFR-TS74 construct upstream of the *TgENT1* start codon. **B.** PCR validation of the promoter replacement for *TgENT1* in RH cells. (L) 1 kb DNA Ladder; 1) LSD-1752 (5' UTR-F of *TgENT1*) and LSD-37 (DHFR ORF reverse), ~ 1 kb; (2) LSD-38-F (T7S4-F) and LSD-1753 (ORF-R of *TgENT1*), ~380; (3) LSD-1752 (5' UTR of *TgNET1*) and LSD-1753 (ORF-R of *TgENT1*), ~4.5 kb. (4) LSD-1752 (5' UTR-F of *TgENT1*) and LSD-37 (DHFR cassette reverse), no band (5) LSD-38 (T7S4-F) and LSD-1753 (ORF-R of *TgENT1*), no band; (6) LSD-1752F and LSD-1753; band size ~280 bp. **C.** qRT-PCR of *TgENT1* mRNA after addition of ATc, normalized to the expression of catalase. The amount of cDNA template used was 10 ng. The presented results are the mean and  $\pm$  SEM of 3 independent biological replicates, each performed in triplicate.  $**P < 0.01$  by one sample t-test. **D.** Plaque assay to assess *in vitro* growth of the *TgENT1*-KD strain (left) along with parental control (right) in HFF cells, in the presence and absence of ATc.

### 3.1.6. Expression of TgENTs in a Leishmania Mexicana Cell Line Deficient in Nucleobase Transport

We have previously shown the utility of expressing protozoan ENT-family transporters in *L. mexicana* cell lines that lack either nucleoside transport ( $\Delta$ LmexNT1.1/1.2/2, "SUPKO") or nucleobase transport ( $\Delta$ LmexNT3, "LmexNT3-KO") [31]. Here, we used that same procedure to express *TgENT1* in the *LmexNT3*-KO strain. The *TgENT1* minigene was amplified by PCR from cDNA of the *T. gondii* RH strain and ligated into the *Nde*I and *Xho*I-digested plasmid pNUS-HcN [34] (Figure 5A). *TgENT1* was then ligated into the digested pNUS-HcN using the NEBuilder HiFi DNA Assembly Cloning Kit, creating plasmid pHDK295, and used to transform *E. coli*. Six positive clones were picked and the correct plasmid assembly verified by a diagnostic digestion with *Nde*I and *Xho*I and by PCR for *TgENT1* integration into pHDK295, followed by Sanger sequencing of the amplicon. Upon confirmation of the correct sequence, pHDK295 was transfected into *LmexNT3*-KO and selected on 50  $\mu$ g/mL of G-418. Clones were obtained by limiting dilution and the presence of the plasmid in these clones was confirmed by PCR (Figure 5B). The relative expression level of *TgENT1* in these clones was assessed by qRT-PCR, showing highest expression in clone 2 (Figure 5C), which was therefore used for further analysis of the transporter function (see below).

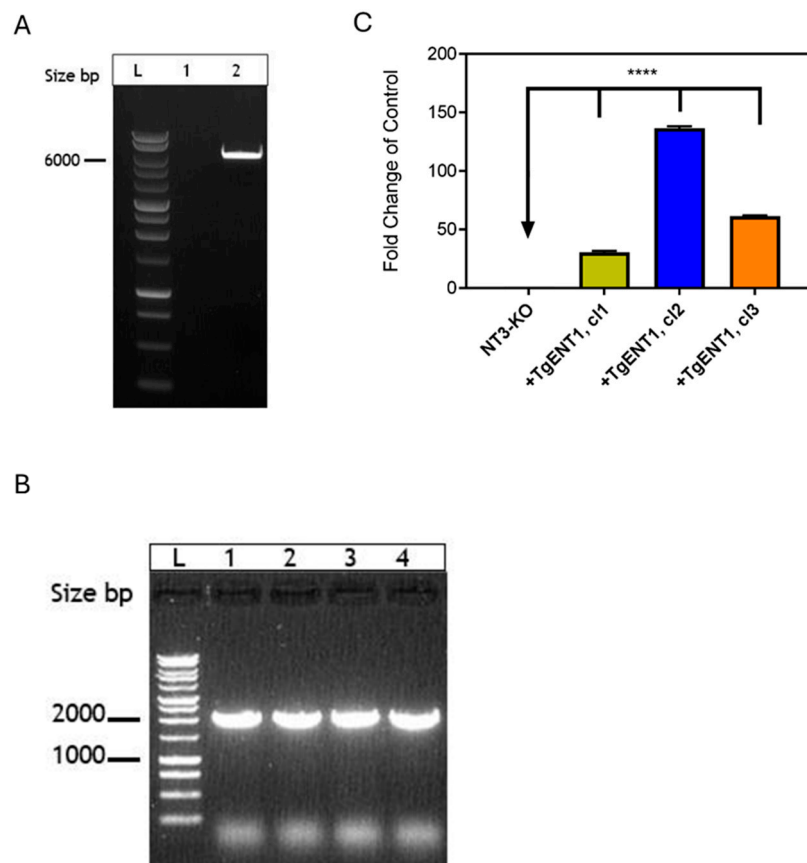


**Figure 5.** Construction of *Leishmania mexicana* cell lines expressing the *TgENT1* minigene. **A.** pNUS-HcN vector digestion by *NdeI* and *XhoI* restriction enzymes run on 1% agarose gel; band size was 6.3 kb. (L) 1 kb DNA Ladder (Promega); (1): Negative control water; (2): digested pNUS-HcN with the size band (6.3 kb). **B.** PCR confirmation of the presence of *TgENT1* minigene in *LmexNT3-KO* clones grown out after transfection with pNUS/*TgENT1* and selection on G-418; *TgENT1*-specific forward primer HDK-1739 and reverse primer (3' vector sequence) HDK-340. (L) 1 kb DNA Ladder (Promega); (1): Clone1; (2): clone2; (3): clone3; (4): clone 4 (~2.2 kb). **C.** The expression levels of *TgENT1* in *Lmex-NT3-KO* and compared to the control (*LmexNT3-KO*) determined by qRT-PCR; expression levels in three independent clones is shown.

### 3.2. Investigation into the Physiological Role of the *TgENT* Transporters

#### 3.2.1. Is *TgENT2* or *TgENT3* Involved in Pyrimidine Uptake in *T. gondii*?

Messina et al. [26] reported that *TgAT1* and *TgENT3* gene products are important in bradyzoite formation and thus for persistence of *T. gondii* in the host. Several authors also demonstrated that *TgENT1* is essential in tachyzoites [26,46,47]. However, the role of the individual transport proteins in *T. gondii* physiology is poorly defined. We have recently reported the identification of a uracil/uridine transporter, *TgUUT*, in *T. gondii* tachyzoites [13] that is potentially important for anti-toxoplasma chemotherapy development. Our starting point was therefore to try to establish which of the four *TgENT* genes encodes this pyrimidine transporter, using the knockout and knockdown lines we generated.

As the *TgAT1* gene product has already been characterized as a purine-specific transporter [24,25] and *TgENT1* is essential and thus harder to manipulate, we first performed uridine transport assays with the knockout strains of *TgENT2* and *TgENT3* (Section 1.2) in parallel with the parental strain as a control. Figure 6A shows that the two knockout strains displayed identical rates of uridine uptake, although both showed an apparently lower rate than the control and requiring us to investigate uridine uptake in both strains in detail.

The knockout strain *TgENT2-KO* displayed robust uptake of 0.1  $\mu\text{M}$  [ $^3\text{H}$ ]-uridine, with an average  $K_m$  of  $5.29 \pm 0.58 \mu\text{M}$  and a  $V_{\text{max}}$  of  $0.025 \pm 0.02 \text{ pmol}(10^7 \text{ cells})^{-1}\text{min}^{-1}$  (Figure 6B), which is not significantly different from the corresponding values in the parental cell line (Table 2). Indeed, the inhibition constants for uracil, inosine and adenosine were also highly similar to the parental line (Figure 6C, Table2;  $P > 0.05$ ). The same pattern was observed with the *TgENT3-KO* (Figure 6D,E) and Table 2 lists the three sets of parameters side-by-side. The data allowed for two possible hypotheses: (a) neither gene encodes the *TgUUT1* uridine/uracil transporter, or (b) they both express a highly similar uridine/uracil transporter and only the knockout of both genes simultaneously would create a cell line that was deficient in the uptake of these pyrimidines. The *TgENT2/3dKO* strain (Section 1.3) allowed us to distinguish between these possibilities. Figure 6F shows that uridine uptake was identical in *TgENT2/3dKO* and parental cells, and Figure 6G shows that uracil uptake was somewhat higher in the dKO cells – certainly not lower. Overall, these data show that neither *TgENT2* nor *TgENT3* encode the *TgUUT1* pyrimidine transport activity.

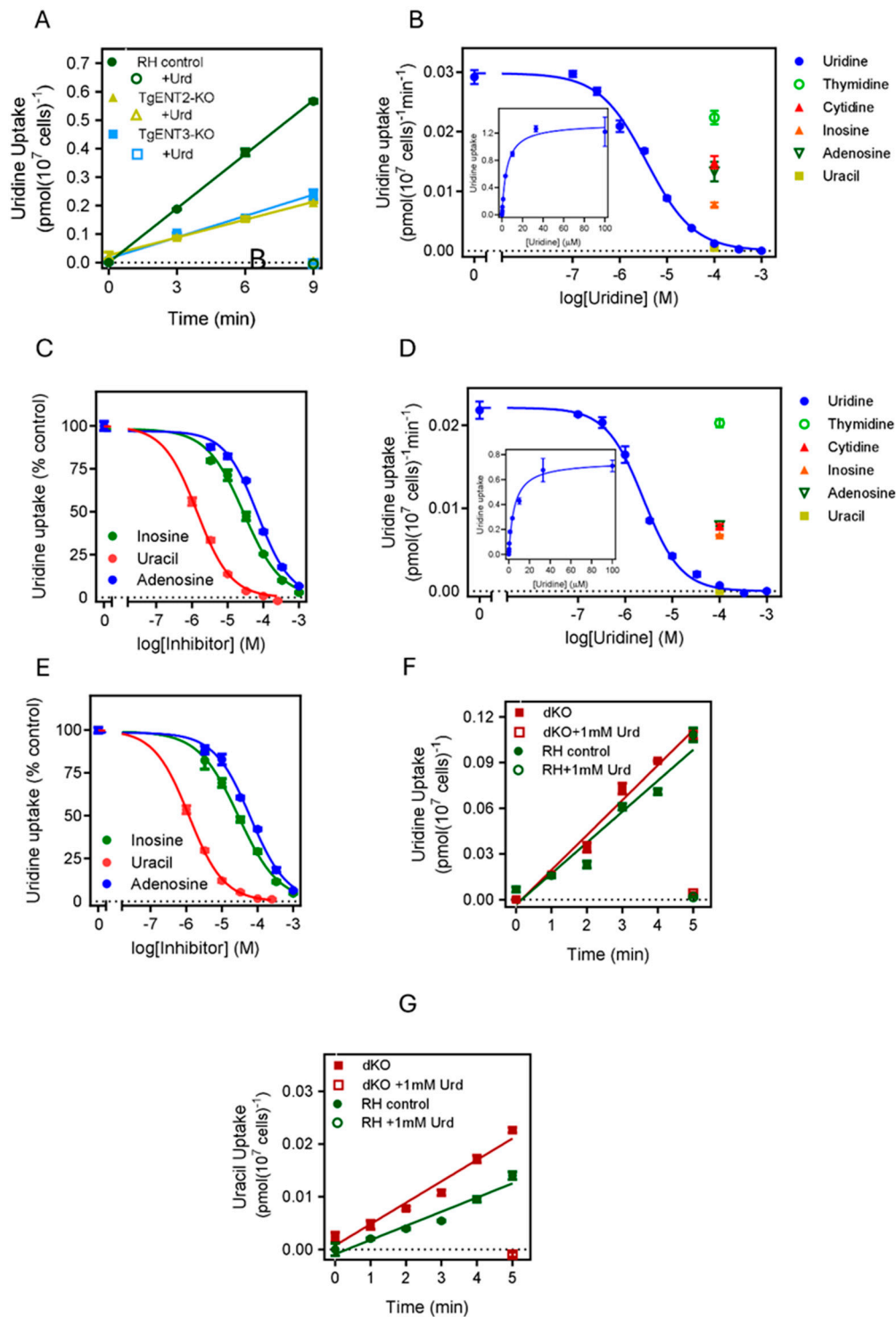


**Figure 6.** Pyrimidine transport in tachyzoites of the *TgENT2* and *TgENT3* knockout strains. **A.** Time course of  $0.1 \mu\text{M}$  [ $^3\text{H}$ ]-uridine transport by the indicated strains in the absence (0, 3, 6 and 9 min) or presence (9 min) of  $1 \text{ mM}$  unlabeled uridine. **B/D.** Dose-response inhibition of unlabeled uridine or of  $100 \mu\text{M}$  of other purines and pyrimidines of  $0.1 \mu\text{M}$  [ $^3\text{H}$ ]-uridine transport by *TgENT2*-KO and *TgENT3*-KO cells respectively. *Inset*: conversion of the uridine inhibition data to a Michaelis-Menten saturation curve. **C./E.** Dose-dependent inhibition of  $0.1 \mu\text{M}$  [ $^3\text{H}$ ]-uridine transport by *TgENT2*-KO and *TgENT3*-KO cells by uracil respectively, inosine and adenosine; expressed as % of uninhibited control. **F.** Timecourse of  $0.1 \mu\text{M}$  [ $^3\text{H}$ ]-uridine transport by *TgENT2/3dKO* and RH tachyzoites. **G.** As frame F but  $0.1 \mu\text{M}$  [ $^3\text{H}$ ]-uracil transport.

**Table 2.** Kinetic parameters of uridine transport in three cell lines.

	TgENT2-KO	TgENT3-KO	RH <sup>1</sup>	
K <sub>m</sub>	5.29 ± 0.58	3.78 ± 0.92	3.34 ± 0.82	μM
V <sub>max</sub>	0.025 ± 0.002	0.011 ± 0.002	0.020 ± 0.004	pmol(10 <sup>7</sup> cells) <sup>-1</sup> min <sup>-1</sup>
Uracil K <sub>i</sub>	0.96 ± 0.17	1.06 ± 0.14	1.15 ± 0.07	μM
Inosine K <sub>i</sub>	32.2 ± 3.3	37.7 ± 3.82	28.2 ± 4.1	μM
Adenosine K <sub>i</sub>	77.4 ± 10.7	58.9 ± 1.10*	111 ± 6	μM

All values are average ± SEM for n ≥ 3. \*, P = 0.002 in unpaired t-test, relative to RH; all other values were not significantly different from the parental control. <sup>1</sup>values for the control RH cell line were taken from [13] for comparison.

### 3.2.1. Investigating the Role of TgENT1 in Pyrimidine Transport

As the *TgENT1* gene could not be deleted, its role in pyrimidine salvage by tachyzoites was investigated using the promotor replacement line (section 1.4), with expression suppressed upon addition of ATc. As the level of mRNA depletion was almost maximal at 24 h (Figure 4D) and there is a risk of secondary effects on other cellular processes the longer the essential gene is suppressed, transport was assessed at 24 h and at 48 h, and the rates in the presence and absence of ATc compared.

The uptake of 0.1 μM [<sup>3</sup>H]-uridine was highly significantly reduced in *TgENT1*-KD cells incubated for either 24 h or 48 h with ATc, to 62.7% of control (P < 0.0001, F-test) or 66.5% of control (P = 0.0004), respectively; the linear regression slopes of the 24 h and 48 h knockdown lines were not significantly different from each other (P > 0.05) (Figure 7A). Similarly, uptake of 0.1 μM [<sup>3</sup>H]-uracil was significantly lower after incubation with ATc for 24 h (63.8% of control, P = 0.0063) or 48 h (47.4% of control, P = 0.0048) (Figure 7B). As a control, we conducted the same experiment also with 0.1 μM [<sup>3</sup>H]-tryptophan, and in this case the incubation with ATc for either 24 h or 48 h did not affect the rate of uptake (Figure 7C). We thus conclude that the suppression of *TgENT1* mRNA production specifically diminishes the transport of uridine and uracil in tachyzoites.

For further verification we next expressed *TgENT1* in our recently described *Leishmania mexicana* NT3-KO strain (Section 1.5), which displays a null background for purine nucleobase transport and a very low background for uracil uptake, exactly as described for the *Trypanosoma vivax* NT3 nucleobase transporter [31] and the *T. cruzi* NB1 adenine transporter [33]. Expressed from an episome in this system, the *TgENT1* gene product was able to significantly increase 0.1 μM [<sup>3</sup>H]-uracil transport over the background, in a time-dependent fashion, in all three independently generated clones expressing the transporter (Figure 7D). As a further control we assessed the uptake of [<sup>3</sup>H]-adenine in the same *TgENT1*-expressing clones, for which the *LmexNT3*-KO cells give an exceptionally sensitive system, as *L. mexicana* adenine uptake in those cells was only 1.9% and 1.6% of control at 30 s and 60 s incubation time, respectively, in the *L. mexicana*-Cas9 T7 strain [29] that is the parent line of *LmexNT3*-KO [31] (Figure 7E). [<sup>3</sup>H]-adenine was just-detectable and very slightly elevated in two out of the three *TgENT1*-expressing clones tested at each timepoint but remained <3% of the rate in cas9 cells (Figure 7E). However, the data indicate that *TgENT1* has a much higher capacity for uracil uptake than for adenine uptake. The combined data with the *TgENT1*-KD tachyzoites and the expression of *TgENT1* in *L. mexicana* NT3-KO cells strongly suggest that *TgENT1* encodes TgUUT1.

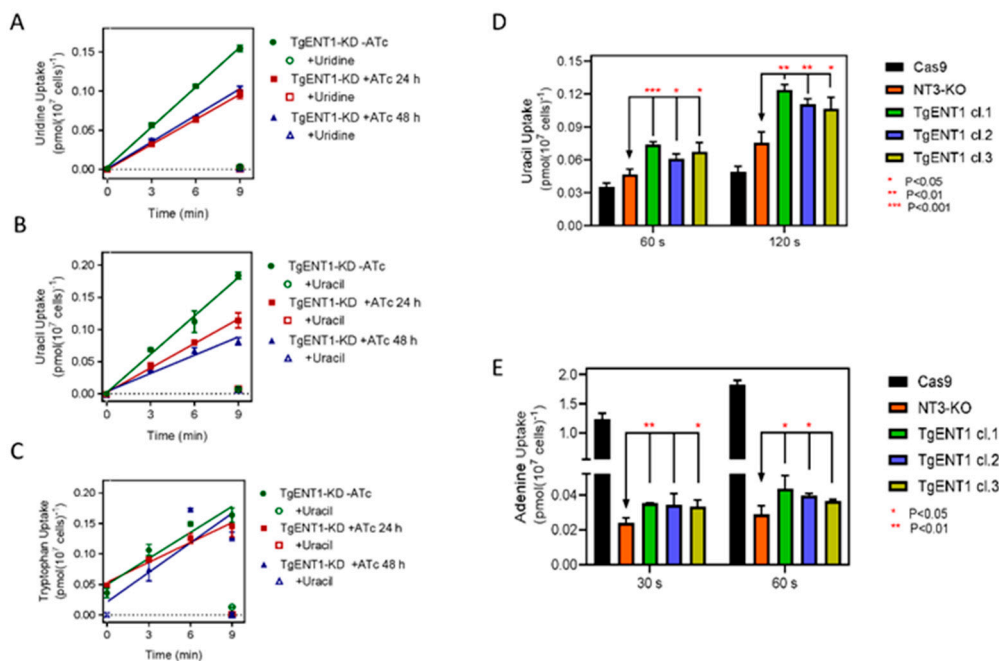


**Figure 7.** *TgENT1* is a pyrimidine transporter. **A/B/C.** Transport of 0.1  $\mu\text{M}$  [ $^3\text{H}$ ]-uridine, 0.1  $\mu\text{M}$  of [ $^3\text{H}$ ]-uracil or [ $^3\text{H}$ ]-tryptophan respectively, by *T. gondii* tachyzoites engineered with promoter replacement for the suppression of *TgENT1* expression in the presence of anhydrous tetracycline (ATc). Cells were cultured in the presence of ATc for either 24 h or 48 h prior to the uptake experiment and then compared to cells cultured in the absence of ATc (green circles); for each category uptake was also measured at 9 min of incubation in the presence of 1 mM unlabeled substrate (uridine, Urd). **D.** Uptake of 0.1  $\mu\text{M}$  of [ $^3\text{H}$ ]-uracil by *L. mexicana* NT3-KO promastigotes expressing the *TgENT1* minigene. Cas9 is the parental strain of NT3-KO, i.e. does express the *LmexNT3* nucleobase transporter. Three independent clones of NT3/*TgENT1* were assessed, each in triplicate. **E.** As frame D but with 0.1  $\mu\text{M}$  [ $^3\text{H}$ ]-adenine.

### 3.3. Effect of Transporter Knockouts on Sensitivity to 5-Fluorinated Pyrimidines

If the above conclusion, that *TgENT1* is likely to be the gene encoding the *TgUUT1* uracil/uridine uptake activity, is correct, then sensitivity to pyrimidine antimetabolites such as 5F-uracil, 5F-uridine and 5F-2'-deoxyuridine, all potent agents against *T. gondii* *in vitro* [13], should not vary with the expression levels of the other three *TgENTs*.

All three pyrimidine analogues that were screened in our previous study [13] showed good activity against *T. gondii* RH with a cytostatic effect at lower concentrations and a cytotoxic effect at high concentrations against HFF monolayer cells. The best activity was displayed by 5-fluorouridine, with an  $\text{EC}_{50}$  of 0.45  $\mu\text{M}$ , 27.6-fold lower than for the standard drug sulfadiazine (Table 3).

The pyrimidine analogues displayed essentially the same activity against the knockout strains of *TgENT2*, *TgENT3* and *TgAT1*, with the sole exception of a just-significant sensitization by the *TgENT2*-KO strain to 5F-uridine ( $\text{EC}_{50} = 0.33 \mu\text{M}$ ;  $P = 0.02$ ) and with a similar trend in *TgENT3* cells that did not reach significance ( $\text{EC}_{50} = 0.36 \mu\text{M}$ ;  $P = 0.07$ ). In the double knockout strain that  $\text{EC}_{50}$  value further decreased to 0.29  $\mu\text{M}$  ( $P = 0.003$ ) and the values for 5F-uracil and 5F-2'-deoxyuridine were also significantly lower. This trend could be due to a possible upregulation in the pyrimidine salvage pathways or perhaps the internal distribution of pyrimidine metabolites in the cell. The observations with the 5F-pyrimidine antimetabolites are fully consistent with *TgAT1*, *TgENT2* and *TgENT3* having no significant role in uracil and uridine transport. Unfortunately, it was not possible to test 5F-pyrimidine sensitivity on a *TgENT1*-KO, which we could not isolate as it is lethal, nor with the knockdown line which shows an early growth arrest, as the assay requires a healthy, growing cell population.

## 4. Discussion

In this study we aimed to identify the gene encoding the *T. gondii* uracil/uridine transporter TgUUT1 that we recently described in isolated tachyzoites [13]. Tachyzoites with a disrupted pyrimidine biosynthesis pathway (i.e. auxotrophs) are able to grow *in vitro* on uracil or uridine as the sole pyrimidine source [12] but not on thymidine, as the species lack thymidine kinase [50] and is unable to take up [<sup>3</sup>H]-thymidine [13]. The lack of thymidine salvage makes *Toxoplasma*, like *Plasmodium* species, particularly sensitive to antifolates, which are the first-line treatment for toxoplasmosis, as the parasite relies completely on the synthesis of thymidine from 2'-deoxyuridine by folate-dependent thymidylate synthase. [12]. The lack of thymidine kinase similarly underpins the remarkable sensitivity to 5F-uracil, 5F-uridine and 5F-2'-deoxyuridine as their mode of action as the metabolite 5F-2'-deoxyuridine monophosphate (5F-dUMP) inhibits thymidylate synthase, and 5F-2'-dUTP is incorporated in place of TTP into nucleic acids, leading to growth arrest and fatal DNA damage, respectively [51]. The reliance on thymidylate synthase is shared with the related *Plasmodium* species as these are also unable to take up thymidine [44], yet *Plasmodium* are very much less sensitive to 5F-uracil, 5F-uridine and 5F-2'-deoxyuridine but highly sensitive to 5F-orotate [52] as, unlike *T. gondii* [13], orotate is the only pyrimidine they are able to take up or incorporate into their nucleic acids [53,54]. This provides a demonstration for the importance of transporters in the effectiveness of fluorinated pyrimidines and other antimetabolites.

In agreement with other recent reports [26,46] we identified four potential nucleoside transporter genes in the *Toxoplasma* genomes available on toxoDB.org, all of the ENT family. Of these, we have previously characterized TgAT1 in great detail and shown that it encodes a high affinity purine transporter with no measurable affinity for uracil and uridine [25]. As TgUUT1 displays high affinity for both uracil and uridine, and low affinity at best for purine nucleosides [13], TgAT1 does not encode the uracil/uridine transporter. In the current study we made gene deletion strains for TgENT2 and TgENT3 as well as the double knockout TgENT2/3dKO and showed that these deletions did not materially change [<sup>3</sup>H]-uridine uptake parameters or reduce sensitivity to 5F-pyrimidines leading us to conclude that neither of these genes encode the TgUUT1 activity either, leaving TgENT1 as the most likely candidate.

As the gene could not be deleted [26] we created a cell line where its expression is controlled by the tetracycline responsive promoter T754 and thus suppressed in the presence of ATc. As expected, the abundance of the corresponding mRNA was reduced by >80% at 24 h, 48 h and 72 h. In order to minimize any secondary effects from the knockdown we assessed the uptake of 0.1 μM [<sup>3</sup>H]-uridine or 0.1 μM uracil at 24 h and 48 h and compared the rate in the presence and absence of ATc. The uptake rate for both substrates, and at both timepoints, was highly and significantly reduced, while the rate of uptake of 0.1 μM [<sup>3</sup>H]-tryptophan was unaffected. Moreover, the expression of TgENT1 in a *Leishmania* cell line with a low endogenous rate of uracil uptake increased uptake of 0.1 μM [<sup>3</sup>H]-uracil significantly in all three independent clones assayed while barely affecting [<sup>3</sup>H]-adenine uptake rates despite the near-zero uptake level for the purine nucleobase.

The combined data presented strongly suggest that TgENT1 encodes the TgUUT1 uracil/uridine transport activity. Certainly, we have conclusively shown, in this and our previous paper [13], that none of the other TgENTs are involved in uracil or uridine uptake. Logically, however, that leaves the possibility of a non-ENT family transporter to be also involved in this process. Such a hypothetical transporter is unlikely to be of the CNT family either, nor of any of the other known nucleobase or nucleoside transporter families [14,55] as, to the best of our knowledge, no members of any of these gene families have to date been identified in protozoan genomes. However, it should be noted here that the genes encoding the high affinity uracil transporters of *Leishmania* [56] and *Trypanosoma* species [57,58] have not yet been identified and we have speculated that they may be encoded by a different, as yet unknown transporter family [59]. However, these kinetoplastid transporters are extremely selective for uracil only whereas TgUUT1 displays identical affinity for uracil and uridine [13]. Substantial efforts from our group [60,61] and the group of Marc Ouellette [62] have not identified any such novel transporter in kinetoplastids.

In conclusion, we believe that *TgENT1* encodes the *T. gondii* uracil/uridine transporter TgUUT1, responsible for the uptake of 5F-pyrimidines with high activity against this parasite. Since the TgENT1 transport activity is essential, as is the thymidine synthase pathway that mediates the action of these compounds, its use would not be expected to lead to rapid onset of resistance.

**Table 3.** *In vitro* drug screening and HFF cytotoxicity using pyrimidine nucleobase and nucleoside analogues on different cell lines of *T. gondii* RH intracellular tachyzoites, TgAT1-KO, TgENT1-KO, TgENT2-KO and TgENT2/3dKO.

ID	RH			TgAT1-KO			TgENT2-KO			TgENT3-KO			TgENT2/3dKO			HFF cytotoxicity		
	EC <sub>50</sub> ± SEM <sup>a</sup>	EC <sub>50</sub> ± SEM	P <sup>b</sup>	EC <sub>50</sub> ± SEM	P <sup>b</sup>	EC <sub>50</sub> ± SEM	P <sup>b</sup>	EC <sub>50</sub> ± SEM	P <sup>b</sup>	EC <sub>50</sub> ± SEM	P <sup>b</sup>	EC <sub>50</sub> ± SEM	P <sup>b</sup>	EC <sub>50</sub> Cytostatic <sup>a</sup>	EC <sub>50</sub> Cytocidal <sup>a</sup>	SI		
5-FU	1.13 ± 0.16	0.70 ± 0.21	0.17	1.36 ± 0.26	0.49	0.82 ± 0.24	0.34	0.51 ± 0.08	0.03	2.49 ± 0.43	3074 ± 339	2720						
5-FUrd	0.45 ± 0.02	0.89 ± 0.42	0.35	0.33 ± 0.02	0.02	0.36 ± 0.03	0.07	0.29 ± 0.002	0.003	0.11 ± 0.10	20.4 ± 1	45						
5-F-2'dUrd	0.67 ± 0.07	0.41 ± 0.14	0.16	0.84 ± 0.07	0.14	0.56 ± 0.07	0.28	0.40 ± 0.06	0.04	0.19 ± 0.05	1478 ± 512	2205						
Sulfadiazine	12.4 ± 1.08	3.95 ± 0.29	0.0003	7.15 ± 0.19	0.01	8.12 ± 0.22	0.02	5.74 ± 0.29	0.004	--	--	--						
PAO	--	--	--	--	--	--	--	--	--	--	0.06 ± 0.003							

All EC<sub>50</sub> values are averages and SEM of at least three independent experiments, given in μM. SI, selectivity index (HFF cytotoxic EC<sub>50</sub>/RH EC<sub>50</sub>). PAO. <sup>a</sup>Values taken from [13]. <sup>b</sup>P value is based on an unpaired Student t-test (RH EC<sub>50</sub> versus knockout *TgENT* gene EC<sub>50</sub>).

**Supplementary Materials:** The following supporting information can be downloaded at the website of this paper posted on Preprints.org, Table S1: PCR master mix for Phusion High-Fidelity DNA Polymerase; Table S2: The PCR condition for Phusion High-Fidelity DNA Polymerase; Table S3: Primers for TgENT1 ligation into pNUS-HcN and post-transfection integration confirmation in *L. mex* NT3-KO; Table S4: sgRNA primers for generating knockouts (TgENT2, TgENT3, TgAT1, Knockdown of TgENT1, and DK in (TgENT3) in *T. gondii*; Table S5: List of primers designed and used for generation and confirmation of TgAT1-KO, TgENT1, TgENT2, TgENT3 and DK (ΔTgENT2/3); Table S6: Platinum SuperFi™ Green PCR Master Mix; Table S7: PCR (SuperFi™) program; Table S8: GoTaq G2 Hot Start Green Master Mix DNA Polymerase; Table S9: PCR conditions for GoTaq DNA Polymerase; Table S10: List of primers designed and used in qRT-PCR.

**Author Contributions:** Conceptualization, H.P.dK.; methodology: L.S., M.F.S.; investigation, H.A.A.E., M.F.S.; formal analysis, H.A.A.E., L.S., H.P.dK.; resources: L.S., H.P.dK.; writing—original draft preparation, H.A.A.E., H.P.dK.; writing—review and editing, H.A.A.E., L.S., H.P.dK.; supervision, L.S., H.P.dK.; funding acquisition, L.S., H.P.dK.

**Funding:** This research was funded by a Wellcome Investigator Award (217173/Z/19/Z) and a Wellcome Discovery Award (310879/Z/24/Z)(to L.S.). HE was supported by a studentship from the government of Libya.

**Data Availability Statement:** All relevant data are contained in the manuscript and the supplementary materials.

**Acknowledgments:** We thank the Cellular Analysis Facility from MVLS SRF for their support and assistance with the flow cytometry work. We thank the ToxoDB team (<https://toxodb.org>) and the community contributors for enabling genome mining for *Toxoplasma gondii*.

**Conflicts of Interest:** The authors declare no conflicts of interest.

## Abbreviations

The following abbreviations are used in this manuscript:

ENT	Equilibrative Nucleoside Transporter
TgUUT1	<i>Toxoplasma gondii</i> Uracil/Uridine Transporter 1
TgAT1	<i>Toxoplasma gondii</i> Adenosine Transporter 1

## References

1. Dubey, J.; Murata, F.; Cerqueira-Cézar, C.; Kwok, O.; Villena, I. Congenital toxoplasmosis in humans: an update of worldwide rate of congenital infections. *Parasitology* **2021**, *148*, 1406-1416. doi: 10.1017/S0031182021001013
2. Montoya, J.G.; Liesenfeld, O. Toxoplasmosis. *Lancet* **2004**, *363*, 1965-1976, doi:10.1016/S0140-6736(04)16412-X.
3. Kim, K.; Weiss, L.M. *Toxoplasma gondii*: the model apicomplexan. *Int J Parasitol* **2004**, *34*, 423-432, doi:10.1016/j.ijpara.2003.12.009.
4. Boothroyd, J.C. Expansion of host range as a driving force in the evolution of *Toxoplasma*. *Mem Inst Oswaldo Cruz* **2009**, *104*, 179-184. doi: 10.1590/s0074-02762009000200009
5. El Kouni, M.H.; Guarcello, V.; Al Safarjalani, O.N.; Naguib, F.N. Metabolism and selective toxicity of 6-nitrobenzylthioinosine in *Toxoplasma gondii*. *Antimicrob Agents Chemother* **1999**, *43*, 2437-2443, doi:10.1128/AAC.43.10.2437.
6. Counihan, N.A.; Modak, J.K.; de Koning-Ward, T.F. How malaria parasites acquire nutrients from their host. *Front Cell Dev Biol* **2021**, *9*, 649184. doi: 10.3389/fcell.2021.649184
7. Schwab, J.; Beckers, C.; Joiner, K. The parasitophorous vacuole membrane surrounding intracellular *Toxoplasma gondii* functions as a molecular sieve. *Proc Natl Acad Sci USA* **1994**, *91*, 509-513. doi: 10.1073/pnas.91.2.509
8. Bitew, M.A.; Gaete, P.S.; Swale, C.; Maru, P.; Contreras, J.E.; Saeij, J.P.J. Two *Toxoplasma gondii* putative pore-forming proteins, GRA47 and GRA72, influence small molecule permeability of the parasitophorous vacuole. *mBio* **2024**, *15*, e0308123, doi:10.1128/mbio.03081-23.
9. Berens, R.L.; Krug, E.C.; Marr, J.J. Purine and pyrimidine metabolism. In *Biochemistry and molecular biology of parasites*; Elsevier: 1995; pp. 89-117.
10. Ngo, H.M.; Ngo, E.O.; Bzik, D.J.; Joiner, K.A. *Toxoplasma gondii*: are host cell adenosine nucleotides a direct source for purine salvage? *Exp Parasitol* **2000**, *95*, 148-153, doi:10.1006/expr.2000.4519.
11. De Koning, H.P.; Al-Salabi, M.I.; Cohen, A.M.; Coombs, G.H.; Wastling, J.M. Identification and characterisation of high affinity nucleoside and nucleobase transporters in *Toxoplasma gondii*. *Int J Parasitol* **2003**, *33*, 821-831, doi:10.1016/s0020-7519(03)00091-2.
12. Fox, B.A.; Bzik, D.J. De novo pyrimidine biosynthesis is required for virulence of *Toxoplasma gondii*. *Nature* **2002**, *415*, 926-929. doi: 10.1038/415926a
13. Elati, H.A.; Goerner, A.L.; Martorelli Di Genova, B.; Sheiner, L.; De Koning, H.P. Pyrimidine salvage in *Toxoplasma gondii* as a target for new treatment. *Frontiers in Cellular and Infection Microbiology* **2023**, *13*, 1320160. doi: 10.3389/fcimb.2023.1320160
14. Campagnaro, G.D.; De Koning, H.P. Purine and pyrimidine transporters of pathogenic protozoa—conduits for therapeutic agents. *Medicinal Research Reviews* **2020**, *40*, 1679-1714. doi: 10.1002/med.21667
15. Natto, M.J.; Miyamoto, Y.; Munday, J.C.; AlSiari, T.A.; Al-Salabi, M.I.; Quashie, N.B.; Eze, A.A.; Eckmann, L.; De Koning, H.P. Comprehensive characterization of purine and pyrimidine transport activities in *Trichomonas vaginalis* and functional cloning of a trichomonad nucleoside transporter. *Mol Microbiol* **2021**, *116*, 1489-1511, doi:10.1111/mmi.14840.
16. Aldfer, M.M.; Alfayez, I.A.; Elati, H.A.; Gayen, N.; Elmahallawy, E.K.; Milena Murillo, A.; Marsiccobetre, S.; Van Calenbergh, S.; Silber, A.M.; De Koning, H.P. The *Trypanosoma cruzi* TcrNT2 Nucleoside Transporter Is a Conduit for the Uptake of 5-F-2'-Deoxyuridine and Tubercidin Analogues. *Molecules* **2022**, *27*. doi: 10.3390/molecules27228045
17. Ungogo, M.A.; Aldfer, M.M.; Natto, M.J.; Zhuang, H.; Chisholm, R.; Walsh, K.; McGee, M.; Ilbeigi, K.; Asseri, J.I.; Burchmore, R.J.S.; et al. Cloning and Characterization of *Trypanosoma congolense* and *T. vivax* Nucleoside Transporters Reveal the Potential of P1-Type Carriers for the Discovery of Broad-Spectrum Nucleoside-Based Therapeutics against Animal African Trypanosomiasis. *Int J Mol Sci* **2023**, *24*, 3144, doi:10.3390/ijms24043144.
18. Young, J.D. The SLC28 (CNT) and SLC29 (ENT) nucleoside transporter families: a 30-year collaborative odyssey. *Biochem Soc Trans* **2016**, *44*, 869-876, doi:10.1042/BST20160038.

19. Delespaux, V.; de Koning, H.P. Transporters in Anti-Parasitic Drug Development and Resistance. In *Trypanosomatid diseases: molecular routes to drug discovery*; Jäger, T., Koch, O., Flohe, L., Eds.; 2013; pp. 335–349.
20. Munday, J.C.; Settimo, L.; de Koning, H.P. Transport proteins determine drug sensitivity and resistance in a protozoan parasite, *Trypanosoma brucei*. *Front Pharmacol* **2015**, *6*, 32, doi:10.3389/fphar.2015.00032.
21. Dunay, I.R.; Gajurel, K.; Dhakal, R.; Liesenfeld, O.; Montoya, J.G. Treatment of Toxoplasmosis: Historical Perspective, Animal Models, and Current Clinical Practice. *Clin Microbiol Rev* **2018**, *31*, 10.1128/cmr.00057-00017, doi:10.1128/CMR.00057-17.
22. Vodenkova, S.; Buchler, T.; Cervena, K.; Veskrnova, V.; Vodicka, P.; Vymetalkova, V. 5-fluorouracil and other fluoropyrimidines in colorectal cancer: Past, present and future. *Pharmacol Ther* **2020**, *206*, 107447, doi:10.1016/j.pharmthera.2019.107447.
23. Dhiver, C.; Milandre, C.; Poizot-Martin, I.; Drogoul, M.P.; Gastaut, J.L.; Gastaut, J.A. 5-Fluoro-uracil-clindamycin for treatment of cerebral toxoplasmosis. *AIDS* **1993**, *7*, 143-144, doi:10.1097/00002030-199301000-00034.
24. Chiang, C.W.; Carter, N.; Sullivan, W.J., Jr.; Donald, R.G.; Roos, D.S.; Naguib, F.N.; el Kouni, M.H.; Ullman, B.; Wilson, C.M. The adenosine transporter of *Toxoplasma gondii*. Identification by insertional mutagenesis, cloning, and recombinant expression. *J Biol Chem* **1999**, *274*, 35255-35261, doi:10.1074/jbc.274.49.35255.
25. Campagnaro, G.D.; Elati, H.A.A.; Balaska, S.; Martin Abril, M.E.; Natto, M.J.; Hulpia, F.; Lee, K.; Sheiner, L.; Van Calenbergh, S.; de Koning, H.P. A *Toxoplasma gondii* Oxopurine Transporter Binds Nucleobases and Nucleosides Using Different Binding Modes. *Int J Mol Sci* **2022**, *23*, 710, doi:10.3390/ijms23020710.
26. Messina, G.; Goerner, A.; Bennett, C.; Brennan, E.; Carruthers, V.B.; Martorelli Di Genova, B. Impact of equilibrative nucleoside transporters on *Toxoplasma gondii* infection and differentiation. *mBio* **2025**, *16*, e0220725, doi:10.1128/mbio.02207-25.
27. Pittman, K.J.; Aliota, M.T.; Knoll, L.J. Dual transcriptional profiling of mice and *Toxoplasma gondii* during acute and chronic infection. *BMC Genomics* **2014**, *15*, 806, doi:10.1186/1471-2164-15-806.
28. Sheiner, L.; Demerly, J.L.; Poulsen, N.; Beatty, W.L.; Lucas, O.; Behnke, M.S.; White, M.W.; Striepen, B. A systematic screen to discover and analyze apicoplast proteins identifies a conserved and essential protein import factor. *PLoS Pathog* **2011**, *7*, e1002392, doi:10.1371/journal.ppat.1002392.
29. Beneke, T.; Madden, R.; Makin, L.; Valli, J.; Sunter, J.; Gluenz, E. A CRISPR Cas9 high-throughput genome editing toolkit for kinetoplastids. *R Soc Open Sci* **2017**, *4*, 170095, doi:10.1098/rsos.170095.
30. Kabli, A.M.M. Polyomic analyses for rational antileishmanial vaccine development: a role for membrane transporters? PhD thesis, University of Glasgow, 2021.
31. Aldfer, M.M.; AlSiari, T.A.; Elati, H.A.A.; Natto, M.J.; Alfayez, I.A.; Campagnaro, G.D.; Sani, B.; Burchmore, R.J.S.; Diallinas, G.; De Koning, H.P. Nucleoside Transport and Nucleobase Uptake Null Mutants in *Leishmania mexicana* for the Routine Expression and Characterization of Purine and Pyrimidine Transporters. *Int J Mol Sci* **2022**, *23*, 8139, doi:10.3390/ijms23158139.
32. Al-Salabi, M.I.; Wallace, L.J.; De Koning, H.P. A *Leishmania major* nucleobase transporter responsible for allopurinol uptake is a functional homolog of the *Trypanosoma brucei* H2 transporter. *Mol Pharmacol* **2003**, *63*, 814-820.
33. Aldfer, M.M.; Hulpia, F.; van Calenbergh, S.; De Koning, H.P. Mapping the transporter-substrate interactions of the *Trypanosoma cruzi* NB1 nucleobase transporter reveals the basis for its high affinity and selectivity for hypoxanthine and guanine and lack of nucleoside uptake. *Mol Biochem Parasitol* **2024**, *258*, 111616, doi:10.1016/j.molbiopara.2024.111616.
34. Tetaud, E.; Lecuix, I.; Sheldrake, T.; Baltz, T.; Fairlamb, A.H. A new expression vector for *Crithidia fasciculata* and *Leishmania*. *Mol Biochem Parasitol* **2002**, *120*, 195-204, doi:10.1016/s0166-6851(02)00002-6.
35. Curt-Varesano, A.; Braun, L.; Ranquet, C.; Hakimi, M.A.; Bougdour, A. The aspartyl protease TgASP5 mediates the export of the *Toxoplasma* GRA16 and GRA24 effectors into host cells. *Cell Microbiol* **2016**, *18*, 151-167. doi: 10.1111/cmi.12498.
36. Aghabi, D.; Sloan, M.; Gill, G.; Hartmann, E.; Antipova, O.; Dou, Z.; Guerra, A.J.; Carruthers, V.B.; Harding, C.R. The vacuolar iron transporter mediates iron detoxification in *Toxoplasma gondii*. *Nat Commun* **2023**, *14*, 3659, doi:10.1038/s41467-023-39436-y.

37. Ufermann, C.M.; Muller, F.; Frohnecke, N.; Laue, M.; Seeber, F. *Toxoplasma gondii* plaque assays revisited: Improvements for ultrastructural and quantitative evaluation of lytic parasite growth. *Exp Parasitol* **2017**, *180*, 19-26, doi:10.1016/j.exppara.2016.12.015.
38. Ovcariakova, J.; Shikha, S.; Lacombe, A.; Courjol, F.; McCrone, R.; Hussain, W.; Maclean, A.; Lemgruber, L.; Martins-Duarte, E.S.; Gissot, M.; et al. Two ancient membrane pores mediate mitochondrial-nucleus membrane contact sites. *J Cell Biol* **2024**, *223*, e202304075, doi:10.1083/jcb.202304075.
39. Maclean, A.E.; Sloan, M.A.; Renaud, E.A.; Argyle, B.E.; Lewis, W.H.; Ovcariakova, J.; Demolombe, V.; Waller, R.F.; Besteiro, S.; Sheiner, L. The *Toxoplasma gondii* mitochondrial transporter ABCB7L is essential for the biogenesis of cytosolic and nuclear iron-sulfur cluster proteins and cytosolic translation. *MBio* **2024**, *15*, e00872-00824. doi: 10.1128/mbio.00872-24
40. Livak, K.J.; Schmittgen, T.D. Analysis of relative gene expression data using real-time quantitative PCR and the 2<sup>-</sup>ΔΔCT method. *Methods* **2001**, *25*, 402-408. doi: 10.1006/meth.2001.1262
41. Ali, J.A.; Tagoe, D.N.; Munday, J.C.; Donachie, A.; Morrison, L.J.; De Koning, H.P. Pyrimidine biosynthesis is not an essential function for *Trypanosoma brucei* bloodstream forms. *Plos one* **2013**, *8*, e58034. doi: 10.1371/journal.pone.0058034.
42. Pfaffl, M.W. A new mathematical model for relative quantification in real-time RT-PCR. *Nucleic Acids Res* **2001**, *29*, e45, doi:10.1093/nar/29.9.e45.
43. Kang, X.; Szallies, A.; Rawer, M.; Echner, H.; Duszenko, M. GPI anchor transamidase of *Trypanosoma brucei*: in vitro assay of the recombinant protein and VSG anchor exchange. *J Cell Sci* **2002**, *115*, 2529-2539, doi:10.1242/jcs.115.12.2529.
44. De Koning, H.P.; Bridges, D.J.; Burchmore, R.J. Purine and pyrimidine transport in pathogenic protozoa: from biology to therapy. *FEMS Microbiol Rev* **2005**, *29*, 987-1020, doi:10.1016/j.femsre.2005.03.004.
45. Chaudhary, K. *Purine transport and salvage in apicomplexan parasites*; Ph.D thesis, University of Pennsylvania: 2005.
46. Qian, J.; Guo, L.; Yang, Y.; He, Z.; He, M.; Chen, C.; Luo, Y.; Xu, J.; Li, S.; Fang, R. A nucleoside transporter on the mitochondria of *T. gondii* is essential for maintaining normal growth of the parasite. *Parasites & Vectors* **2025**, *18*, 418.
47. Sidik, S.M.; Huet, D.; Ganesan, S.M.; Huynh, M.H.; Wang, T.; Nasamu, A.S.; Thiru, P.; Saeij, J.P.J.; Carruthers, V.B.; Niles, J.C.; et al. A Genome-wide CRISPR Screen in *Toxoplasma* Identifies Essential Apicomplexan Genes. *Cell* **2016**, *166*, 1423-1435 e1412, doi:10.1016/j.cell.2016.08.019.
48. Meissner, M.; Schluter, D.; Soldati, D. Role of *Toxoplasma gondii* myosin A in powering parasite gliding and host cell invasion. *Science* **2002**, *298*, 837-840, doi:10.1126/science.1074553.
49. Lacombe, A.; Maclean, A.E.; Ovcariakova, J.; Tottey, J.; Muhleip, A.; Fernandes, P.; Sheiner, L. Identification of the *Toxoplasma gondii* mitochondrial ribosome, and characterisation of a protein essential for mitochondrial translation. *Mol Microbiol* **2019**, *112*, 1235-1252, doi:10.1111/mmi.14357.
50. Fox, B.A.; Belperron, A.A.; Bzik, D.J. Negative selection of *Herpes simplex* virus thymidine kinase in *Toxoplasma gondii*. *Mol Biochem Parasitol* **2001**, *116*, 85-88, doi:10.1016/s0166-6851(01)00302-4.
51. Longley, D.B.; Harkin, D.P.; Johnston, P.G. 5-fluorouracil: mechanisms of action and clinical strategies. *Nat Rev Cancer* **2003**, *3*, 330-338, doi:10.1038/nrc1074.
52. Rathod, P.K.; Khatri, A.; Hubbert, T.; Milhous, W.K. Selective activity of 5-fluoroorotic acid against *Plasmodium falciparum* in vitro. *Antimicrob Agents Chemother* **1989**, *33*, 1090-1094, doi:10.1128/AAC.33.7.1090.
53. Gutteridge, W.; Trigg, P. Incorporation of radioactive precursors into DNA and RNA of *Plasmodium knowlesi* in vitro. *The J Protozool* **1970**, *17*, 89-96. doi: 10.1111/j.1550-7408.1970.tb05163.x
54. Van Dyke, K.; Tremblay, G.C.; Lantz, C.H.; Szustkiewicz, C. The source of purines and pyrimidines in *Plasmodium berghei*. *Am J Trop Med Hyg* **1970**, *19*, 202-208, doi:10.4269/ajtmh.1970.19.202.
55. De Koning, H.; Diallinas, G. Nucleobase transporters. *Mol Membr Biol* **2000**, *17*, 75-94. doi: 10.1080/09687680050117101
56. Papageorgiou, I.G.; Yakob, L.; Al Salabi, M.I.; Diallinas, G.; Soteriadou, K.P.; De Koning, H.P. Identification of the first pyrimidine nucleobase transporter in *Leishmania*: similarities with the *Trypanosoma brucei* U1 transporter and antileishmanial activity of uracil analogues. *Parasitology* **2005**, *130*, 275-283, doi:10.1017/s0031182004006626.

57. De Koning, H.P.; Jarvis, S.M. A highly selective, high-affinity transporter for uracil in *Trypanosoma brucei*: evidence for proton-dependent transport. *Biochem Cell Biol* **1998**, *76*, 853-858, doi:10.1139/bcb-76-5-853.
58. Gudín, S.; Quashie, N.B.; Candlish, D.; Al-Salabi, M.I.; Jarvis, S.M.; Ranford-Cartwright, L.C.; de Koning, H.P. *Trypanosoma brucei*: a survey of pyrimidine transport activities. *Exp Parasitol* **2006**, *114*, 118-125, doi:10.1016/j.exppara.2006.02.018.
59. De Koning, H.P. Pyrimidine transporters of trypanosomes—a class apart? *Trends in Parasitology* **2007**, *23*, 190.
60. Ali, J.A.M. Pyrimidine salvage and metabolism in kinetoplastid parasites. University of Glasgow, 2013.
61. Alzahrani, K.J.H. Strategies for the identification and cloning of genes encoding pyrimidine transporters of *Leishmania* and *Trypanosoma* species. Ph.D thesis, University of Glasgow, 2017.
62. Ritt, J.F.; Raymond, F.; Leprohon, P.; Legare, D.; Corbeil, J.; Ouellette, M. Gene amplification and point mutations in pyrimidine metabolic genes in 5-fluorouracil resistant *Leishmania infantum*. *PLoS Negl Trop Dis* **2013**, *7*, e2564, doi:10.1371/journal.pntd.0002564.

**Disclaimer/Publisher's Note:** The statements, opinions and data contained in all publications are solely those of the individual author(s) and contributor(s) and not of MDPI and/or the editor(s). MDPI and/or the editor(s) disclaim responsibility for any injury to people or property resulting from any ideas, methods, instructions or products referred to in the content.